Control Strategies for Variable Air Volume Ventilation used as a Demand Response Resource

Ricky Klasson

Johan Frykebrant

LUND UNIVERSITY

Department of Automatic Control

MSc Thesis
TFRT-6108
ISSN 0280-5316

Department of Automatic Control
Lund University
Box 118
SE-221 00 LUND
Sweden

Printed in Sweden by Tryckeriet i E-huset
Lund 2020

Abstract

The Swedish power grid is actively balanced in order to maintain the nominal frequency of 50 Hz. Today, this is mostly done through flexible power generation. Emerging markets, allowing consuming resources to participate in balancing the grid, have the potential to increase the stability of the grid. This master thesis aimed to investigate the consequences and possibilities of using variable air volume (VAV) ventilation systems as a balancing resource for the grid. Through modelling and simulation of these systems, conclusions were drawn regarding the balancing potential. As a consequence of flexible power consumption, VAV room automation was negatively effected. The thesis emphasized development of generic room automation control strategies, reducing negative effects. The main outcome of this thesis was a control strategy which was able to facilitate flexible power consumption whilst retaining close to normal VAV operation. Also, a small economical analysis was performed to give an overview of the potential earnings for balancing resources.

Acknowledgements

We wish to offer special thanks to Kristian Soltesz for his continued support, guidance and for devoting time to supervise the thesis. His knowledge and constructive recommendations for the thesis has challenged the writers whilst keeping the project on track.

We would also like to express our gratitude towards Siemens for giving us the opportunity to conduct the thesis. A special thanks to our supervisor Annah Håkansson, and her colleagues Daniel Iggström and Viktor Persson for laying the foundation for the thesis as well as for the continued support, belief and encouragement throughout. We would also like to thank Mikael Holmberg for his support and education on the ventilation system topic.

Table of Contents

Nomenclature

AHU	**A**ir **H**andling **U**nit
BMS	**B**uilding **M**anagement **S**ystem
DRR	**D**emand **R**esponse **R**esource
FCR-N	**F**requency **C**ontainment **R**eserve - **N**ormal
FCR	**F**requency **C**ontainment **R**eserve
FRR	**F**requency **R**estoration **R**eserve
HVAC	**H**eating **V**entilation and **A**ir **C**onditioning
SvK	**Sv**enska **K**raftnät
TSO	**T**ransmission **S**ystem **O**perator
VAV	**V**ariable **A**ir **V**olume
VFD	**V**ariable **F**requency **D**rive
VPP	**V**irtual **P**ower **P**lant

1

Introduction

1.1 Background

The nominal frequency of the Swedish power grid is 50 Hz. The frequency fluctuates around this value due to a mismatch between production and consumption. Deviations from nominal frequency can damage machinery powered by the grid, cause extra wear on the grid infrastructure and even cause blackouts.

More intermittent production such as wind and solar power and a decrease in continuous production with high inertia, such as nuclear power, is decreasing the stability of the grid frequency. To solve this problem, and maintain a stable grid frequency, the power balance between producers and consumers must be controlled in real time. This is called frequency containment and contributing resources are called demand response resources (DRR).

Up until now, hydro power has been used as the primary DRR in Sweden [NEPP, 2016]. As nuclear power is phased out, hydro power and other energy sources will need to take its place. This may limit the amount of hydro power available for balancing the grid frequency. There is therefore a need to find new candidates, both consumers and producers, that can be used as DRRs.

In 2017, the housing and service sector accounted for 40% of Sweden's total energy consumption, half of which was consumed in the form of electricity [Energimyndigheten, 2019]. This indicates that there is large untapped potential to use electrically powered utilities in buildings as DRRs. Also, many modern buildings are equipped with building management systems (BMS) allowing for control of building utilities. In May 2019, Svenska Kraftnät (SvK) started allowing consuming resources to participate in balancing the grid [Vattenfall, 2019]. Siemens has been at the forefront of research, conducting several master thesis projects on the topic [Iggström and Svensson, 2019] [Persson, 2019]. These theses suggest that building resources such as heating, ventilation and air conditioning (HVAC) could be candidates for flexible power consumption. This thesis analyses the possibilities of using ventilation fans as a balancing resource from a practical point of view.

1.2 Collaboration Project

Siemens has entered a collaboration project with Skandia Fastigheter centered around one of thier buildings: Väla shopping center. Väla is a mall located outside Helsingborg with a vision to reach zero net consumption from the power grid. To reach this goal, Väla has installed solar panels and implemented energy saving measures. Following this, Väla and Siemens are converting Väla into Sweden's first virtual power plant (VPP) [Siemens and Väla, 2020]. A VPP is a network of production and/or consumption resources, such as HVAC systems, batteries and solar panels, whose objective is to relieve the load on the grid by cleverly distributing power during periods of peak load. Previous master theses [Iggström and Svensson, 2019] [Persson, 2019] have identified that ventilation fans consume 20 % of Väla's total electrical energy and suggest that the volume of power consumption and the response time of the fans is sufficient to act as a DRR. The total rated power of all the ventilation fans amount to approximately 1 MW. It is expected that 10-30 % of this can be provided as balancing power.

1.3 Problem Formulation

Prior to this thesis, Siemens had underlined certain problems. These problems are further described and were to be confirmed during simulation. The end goal of the thesis was to solve these problems.

Power Flexibility

For a ventilation fan to act as a DRR, the power consumption must be controlled. Explicit control of the fan power consumption was not implemented at Väla. Hence, the thesis aimed to research the available options for estimating and controlling ventilation fan power consumption.

Room Automation

Explicitly controlling the fan power may create imbalances for underlying systems such as ventilation ducts and indoor climate. The aim was to investigate how these problems manifest themselves and how the system could be adjusted to solve these problems.

1.4 Approach

The goal of this thesis was to identify what limiting factors exist when using ventilation fans as a DRR. Primarily, the thesis sought to develop control strategies for fans and room automation to minimize these limiting factors. Furthermore, the requirements for implementing the proposed solutions were investigated. A generic

ventilation system model with control strategies enabling real time control of the power consumption was developed. Measurements from tests at Väla were used as guidelines for the model. Simulations using this model determined if ventilation fans as a DRR can meet indoor climate requirements.

1.5 Outline

Theory
This chapter covers the theory relevant to the thesis. This includes sections explaining frequency containment, the physical properties of fans and the working principle of a ventilation system and its components.

Method
This chapter covers the method of the thesis in order to understand how the results were achieved. The process of data analysis, site tests, modelling and problem investigation is presented in detail. Furthermore, the development of frequency containment and room automation control strategies is covered. Finally, these strategies are subject to simulations to evaluate performance.

Result
This chapter presents the results from the thesis. First, results from the data analysis are presented. These are followed by presenting the performance test results to compare the developed control strategies to normal operation.

Discussion
This chapter discusses the results of the thesis. The key findings of the thesis are presented followed by the project delimiters. Finally, modelling assumptions, interpretations of results and practical implications are discussed.

Conclusion
This chapter contains a condensed version of the thesis. The approach and key contributions are summarized.

Future work
This chapter suggests topics for future work, building upon the results of this thesis.

2

Theory and Process Model

2.1 Balancing the Power Grid

Long distance transmission of electricity occurs on the national grid. Svenska kraftnät (SvK), the Swedish transmission service operator (TSO) [SvK, 2020a], is responsible for the maintenance and development of the national grid. Another important responsibility of SvK is to keep the grid frequency at 50 Hz. To do this, SvK provides balancing markets where resources are paid to be flexible in their production or consumption, thereby affecting the grid frequency. These markets are split into frequency containment reserve (FCR) markets which are the primary markets, and frequency restoration reserves (FRR) markets which are the secondary markets. The grid is considered to be in normal operation inside the interval 49.9-50.1 Hz. Inside this interval, the frequency is balanced by the FCR-Normal (FCR-N) market [SvK, 2018].

Frequency Containment Reserve - Normal

FCR-N is activated in proportion to the grid frequency deviation inside the interval 49.9-50.1 Hz, according to Figure 2.1. Example: a consuming resource that contributes with 1 MW of balancing power on FCR-N should consume 1 MW less power compared to its nominal level when the frequency is at or below 49.9 Hz and 1 MW more when the frequency is at or above 50.1. Inside the interval 49.9-50.1 Hz, the resource should adjust its power consumption proportionally to the grid frequency deviation.

The smallest amount of balancing power required to participate on FCR-N is 0.1 MW, making it the market with lowest threshold for entry [SvK, 2018]. FCR-N is a symmetric balancing market meaning that a resource must be able to both increase and decrease its power by the amount of balancing power. The total volume of the Swedish FCR-N market amounts to 237 MW [SvK, 2019]. What resources participate on FCR-N any given hour is decided through a bidding process where pricing bids are placed by the resource responsible for the hours it desires to participate. The minimum bid size is 0.1 MW, which is also the step size for bids.

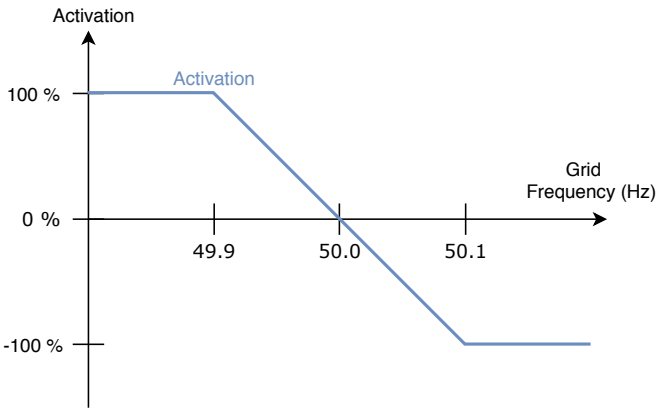

Figure 2.1 Linear activation of FCR-N resource as a function of grid frequency. 100 % activation corresponds to a decrease in power for consuming resources.

The reason for focusing on FCR-N is the fact that requirements for participation are the lowest when compared to other markets. Other markets require faster response time or a very large volume of power flexibility [SvK, 2018].

2.2 Fan Theory

Fan & System Resistance Curves

Fan characteristics can be visualized using fan curves [McLoone, 2019]. The fan curve is produced by allowing the fan to operate at a constant rotational speed in a laboratory setup where the cross-sectional flow area can be varied. Measuring the volume flow rate and the differential pressure over the fan at different cross-sectional areas, a fan curve can be created as in Figure 2.2. Fan curves can be created for several rotational speeds, such as N1 and N2 in the figure, to cover the entire operating range of the fan. Fan curves are usually produced by the fan manufacturer and is the industry standard way of visualizing flow and pressure characteristics of a fan.

The system resistance curve is described by the combinations of pressure and flow that can occur in a given system, as in Figure 2.2. Increasing the restriction in the system by limiting the cross-sectional flow area shifts the curve from R1 to R2, requiring more pressure to produce the same amount of flow. The operating point of the fan is the combination of differential pressure and produced air flow that the fan currently operates at. It is decided by the intersection of the fan curve and the system resistance curve.

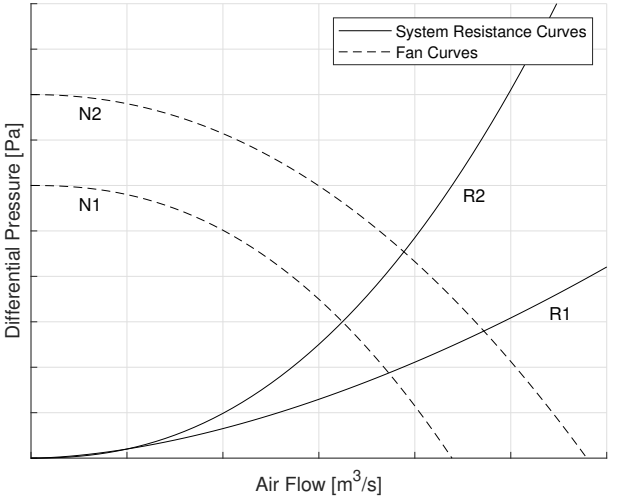

Figure 2.2 A schematic illustration of two fan curves: N1 (low speed) and N2 (high speed), and two system resistance curves: R1 (low resistance) and R2 (high resistance). The intersection of a resistance curve and system curve determines the operating point of the fan.

Affinity Laws

As fans operate, an impeller rotates to produce air flow. The fan also creates a certain pressure differential and draws power. The fan affinity laws govern the relation between these physical properties. These relations are central in understanding the fundamental behaviour of idealised fans when changing some working parameter of the fan.

The following equations [Toolbox, 2003] describe how changes in fan rotational speed N, volume air flow q, differential pressure p and power consumption P are related when altering a parameter from value 1 to 2 if the system resistance is held constant:

$$\frac{q_1}{q_2} = \frac{N_1}{N_2} \tag{2.1}$$

$$\frac{p_1}{p_2} = (\frac{N_1}{N_2})^2 \tag{2.2}$$

$$\frac{P_1}{P_2} = (\frac{N_1}{N_2})^3. \tag{2.3}$$

When varying the rotational speed, the impact on other physical properties can be visualised as in Figure 2.3.

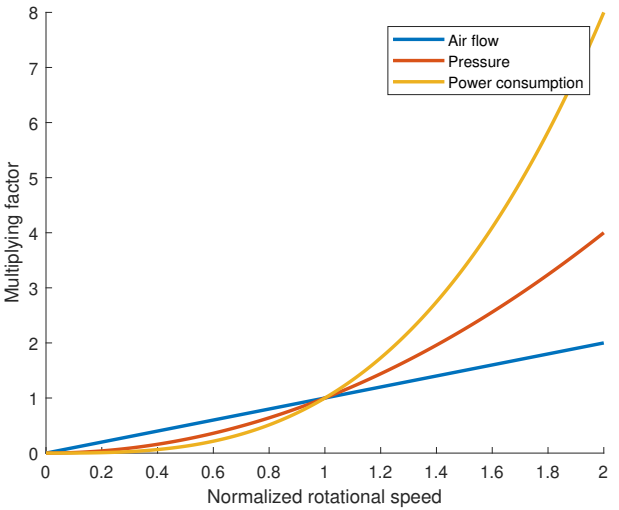

Figure 2.3 Illustration of the effects on flow, pressure and power when varying the rotational speed.

2.3 Ventilation System

Ventilation systems are used to move air into, through and out of building space in order to maintain desirable air quality and temperature. To better understand how a ventilation system is controlled, a rundown of the control structure will follow. Heating of indoor space is generally taken care of by radiators, separate from the ventilation system. Hence, cooling is the primary purpose of ventilation. A ventilation system can be split into three major subsystems: the air handling unit (AHU), the ventilation duct and the rooms supplied by the duct. The presented ventilation system is a variable air volume (VAV) system. Such a system is characterised by the closed loop control of air flow in to each room. Figure 2.4 shows the block diagram of a simplified system. This diagram was constructed for illustrative purposes and does not completely correspond to reality. The individual blocks are further elaborated.

Air Handling Unit

One objective of the AHU is to supply the duct system with air at a desired temperature. This is done by turning large fans, creating a differential pressure to draw air from outdoor. The heating or cooling of the air is excluded in this representation. Also, real world systems may have return air fans and re-circulation dampers which also are omitted.

Pressure Controller, C1
Input: Pressure error [Pa].

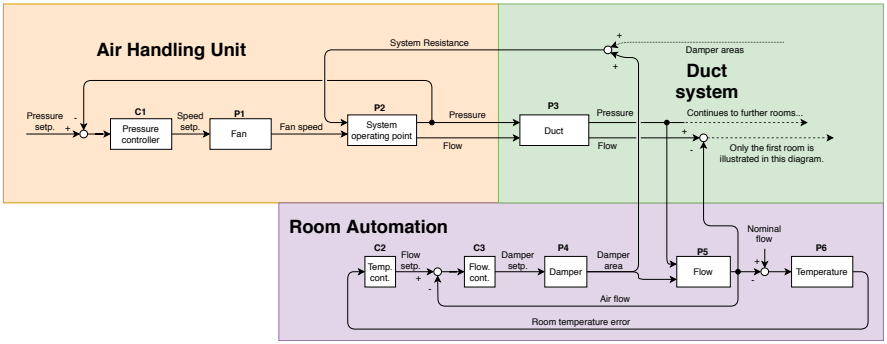

Figure 2.4 Block diagram of a typical, pressure controlled ventilation system with variable air volume (VAV) room automation.

Output: Fan speed setpoint [Hz].
The pressure controller, typically a PI-controller, is used to maintain a desired pressure in the duct. The pressure decreases as air travels downstream. To ensure a positive pressure differential between the rooms and the duct, it is desired to measure and control the duct pressure in a closed loop.

Fan, P1
Input: Fan speed setpoint [Hz].
Output: Fan speed [Hz].
To accurately control the speed of the fan, a variable frequency drive (VFD) is typically used. The output frequency of the VFD decides the speed of the fan. This block has an internal closed speed control loop. The controller is typically a PI-controller. Acceleration and deceleration is limited by the inertia of the fan itself and the maximum allowed current from the VFD.

System Operating Point, P2
Input 1: Fan speed [Hz], Input 2: System resistance $[m^2]$.
Output 1: Fan differential pressure [Pa], Output 2: Flow $[m^3/s]$.
The intersection of the fan curve and the system resistance curve decides the operating point of the fan. The operating point consists of the differential pressure and the flow it produces. How these parameters are affected by a change in fan speed or system resistance is illustrated by the fan curves and system resistance curves in Section 2.2. The individual block P2 depends on the system resistance of the system which, in reality, the duct P3, is part of. However, as the duct dimensions do not change, the system resistance is illustrated to only depend on the damper areas. In reality, the unit of system resistance is not $[m^2]$, but it is thought to be more intuitive.

Duct System

The duct system transports and distributes air received from the AHU to all rooms connected to the duct system. In this model, all rooms are connected to the duct in parallel. The duct ends at the final room.

Duct, P3
Input 1: Duct Pressure [Pa], Input 2: Air Flow $[m^3/s]$.
Output 1: Duct Pressure [Pa], Output 2: Air Flow $[m^3/s]$.
The duct creates resistance in the ventilation system. The resistance depends on the dimensions of the duct as well as the position of the dampers in each room, see Damper, P4.

Room Automation

The purpose of the room automation is to maintain a pleasant indoor air quality. Varying the intake of fresh air into rooms alters the climate. The presented room automation structure is typical for a VAV system, featuring closed loop control of air flow into rooms.

Temperature Controller, C2
Input: Temperature error $[^\circ C]$.
Output: Flow setpoint $[m^3/s]$.
The temperature controller is typically a PI-controller. The output serves as a set point to the flow controller.

Flow Controller, C3
Input: Flow error $[m^3/s]$.
Output: Damper area setpoint $[m^2]$.
The flow controller is typically a P-controller. It decides the position of the damper and can thereby increase or decrease the flow into the room as necessary.

Damper, P4
Input: Damper area setpoint $[m^2]$.
Output: Damper area $[m^2]$.
A damper is a metal plate, positioned inside the duct perpendicular to the flow direction. The damper angle can be altered to vary the cross-sectional flow area and thereby the air flow. Less available flow area increases system resistance and vice versa. The damper has limitations on the speed of which it changes the inlet area to the room.

Flow, P5
Input 1: Duct pressure [Pa], Input 2: Damper area $[m^2]$.
Output: Flow $[m^3/s]$.
The flow process decides the amount of air that flows into the room. It depends on the pressure in the duct where the room inlet is located and the size of the inlet area. The inlet area is determined by the position of the damper.

Temperature, P6
Input: Flow error $[m^3/s]$.
Output: Temperature error $[^\circ C]$.
Throughout this thesis, it is assumed that temperature change is only dependent on the deviation from nominal air flow into the room. Since the ventilation has a cooling effect, more flow results in a decrease in temperature. In reality, the temperature is susceptible to disturbances which are ignored here.

3

Method

3.1 Data Analysis

With the end goal of the thesis in mind, which was to understand the problems of using ventilation fans as a balancing resource for the grid, the first step was to research the behaviour of the grid frequency. The grid frequency is the setpoint signal to FCR-N resources. We therefore sought to understand how the frequency varies and to identify expected operating conditions. Frequency data on which the analysis was performed was taken from the Finnish TSO Fingrid. The data set [Fingrid, 2020] contained raw frequency data from 2015 to 2019, which was sampled at 10 Hz and measured at 400 kV substations in Finland.

Frequency Data Analysis

We formatted the data using Python, and visualized it in Matlab. As the dataset was very large, we preferred to work with a smaller set. By inspecting parts of the dataset it seemed sufficient to work with a sampling frequency of 1 Hz instead of 10 Hz for this general analysis. We performed a spectral analysis on ten randomly selected days throughout the data, all of which showed similar results. The spectral analysis for an example day is shown in Figure 3.1. This figure confirmed that low frequency variations were more pronounced throughout the data since the gain was higher at lower frequencies. We sampled down the data by keeping every tenth sample and then performed the analysis by extracting the grid frequency distribution on a yearly time scale as well as highlighting the distribution of days with deviating average frequency.

Economical Analysis

We used the aforementioned frequency data from Fingrid together with historical pricing data for the FCR-N market [SvK, 2020b] and electricity cost [Nordpool, 2020], to conduct an economical analysis using Matlab. The purpose of the analysis was to find how much annual revenue would have been generated if 1 MW of balancing power was provided every day each year from 2015 to 2019. Also, when

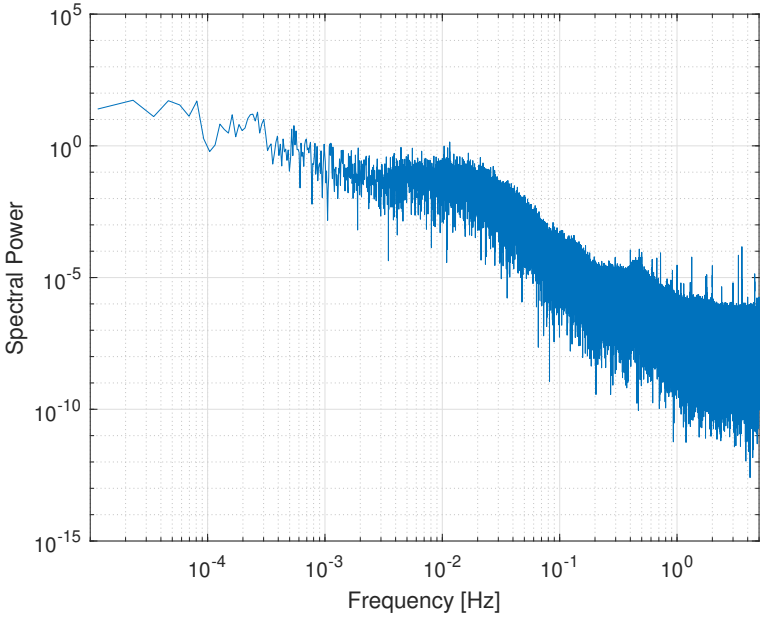

Figure 3.1 Power spectral analysis of the grid frequency. Based on 10 Hz measurement taken on 8th of August 2015. Low frequencies are more pronounced than high frequencies.

DRR resources participate in balancing the grid, the hourly electricity consumption may vary. Hence, we investigated if and by how much the yearly electricity bill of the DRR would change depending on what hours of the day the DRR was active. We performed this analysis using two different electricity prices: one with a constant price, and one for resources with the hourly updated electricity price, known as the spot price. For each hour, we calculated the average balancing power and multiplied it with the electricity price. We then summed these values for the respective years to arrive at the results. The FCR-N revenue was calculated by summing the FCR-N price for each active hour.

3.2 Fan Model

This section and Section 3.3 presents the modelling of the different ventilation subsystems to allow for simulation. We then used this model to investigate problems and to further develop the system. In particular, this section covers the modifications and extensions to the theoretical model in Figure 2.4 needed in order to simulate a fan with flexible power consumption. This part of the modelling resulted in the air handling unit and frequency containment blocks in Figure 3.2.

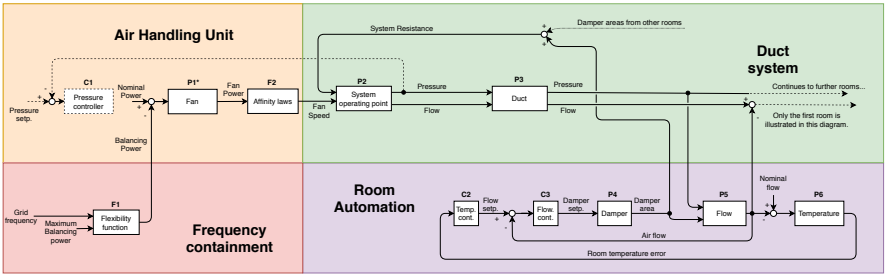

Figure 3.2 Block diagram illustrating the system after power control has been implemented. The pressure controller was disabled. Frequency containment and fan power control was implemented. This system is referred to as System 1.

Fan Power Control

The fan in the base ventilation system model presented in Figure 2.4 was controlled by setting a duct pressure setpoint. There was no way of directly controlling the power consumption of the fan. Frequency containment requires power consumption to follow a reference value. Hence, we investigated different ways of estimating and controlling the power consumption of a fan. These are further elaborated.

Affinity Laws

One option to estimate fan power consumption was to use affinity laws. As presented in Section 2.2, these are relations between air flow, differential pressure, fan speed and power consumption for fans. In a VAV system, the system resistance may change during operation, altering the operating point of the fan, and in extension the power consumption according to Equations 2.1-2.3. Estimating power consumption using affinity laws was further complicated by real world components, such as inlet filters, having varying resistance depending on how clean or dirty they are. Also, mechanical efficiency may vary between systems. Hence, estimating power consumption instead of directly measuring it was deemed too involved and was left outside the scope of this thesis.

Power Measurement

Another option was to physically measure power consumption on site. One caveat for this option was that it may require installation of additional sensors for power measurement. The benefit of this option was the ability to control the fan power in a closed loop which was much more reliable than an open loop estimation using affinity laws. Hence, we assumed the power to be measurable during modelling.

Modelling

We used Simulink models in the analysis and modelling of the system. Figure 3.2 shows the result of the system modelled to facilitate flexible power consumption

without modifications to the room automation. This section covers modelling of the components inside the air handling unit and frequency containment blocks.

Closed Loop Power Dynamics, P1*
Input: Power reference [kW].
Output: Power [kW].
In order to model the power dynamics, we conducted a test at an AHU at Väla. The AHU had a control structure like the AHU in Figure 2.4. During this test we issued a series of steps to the fan speed setpoint directly, noted with "speedsetp." in Figure 2.4, whilst measuring fan speed and power consumption. The pressure controller C1 was disconnected during this test. Figure 3.3 shows the results from this test. The speed follows its setpoint without overshoots while the power consumption has over- and undershoots before settling. This behaviour was expected since the speed was controlled in a closed loop while the power consumption was a result of how the speed was controlled internally in the VFD. By inspecting the test results, we assumed that the closed loop fan speed dynamics could be modelled by a slew rate limit, which limits the acceleration, and a saturation inside 20-50 Hz. It was further assumed that a closed loop power control would act similar to the closed loop speed control. Hence, we modelled the closed loop fan power dynamics, P1*, by limiting the rising and falling slew rates to 1.23 and -0.56 kW/s respectively. We estimated these values from Figure 3.3. Furthermore, in simulation, we set the nominal fan power to 12 kW and the nominal fan speed to 35 Hz. Also, we decided to disable the pressure controller to allow for the power reference signal to be generated by the sum of the nominal power and the balancing power term.

One of the requirements for participating on FCR-N was to meet response time criteria during a step response test [SvK, 2020c, p. 5]. The requirements were to reach 63 % of balancing power within 60 s and 100 % within 180 s, illustrated by Figure 3.4. During the previously mentioned fan test at Väla, shown in Figure 3.3, we evaluated these requirements. The previously estimated falling slew rate was dimensioning as it was lower than the rising slew rate. As the power range of this fan was about 2-38 kW, the maximum flexibility would be 18 kW. The falling slew rate was estimated to -0.56 kW/s. Hence, the maximum time to reach 100 % flexibility was about 32 s, inferring that requirements were met.

Affinity Laws, F2
Input: Fan power [kW].
Output: Fan speed [Hz].
The modelled fan was now controlled with regards to power consumption. Hence, the output of P1* was no longer the fan speed, but instead the power consumption. Since the system operating point P2 required the fan speed as input, we converted the power consumption to a fan speed using affinity laws described in Section 2.2, specifically using Equation 2.3. This was an approximation to simplify modelling. In reality, fan power also depended on the operating point of the fan.

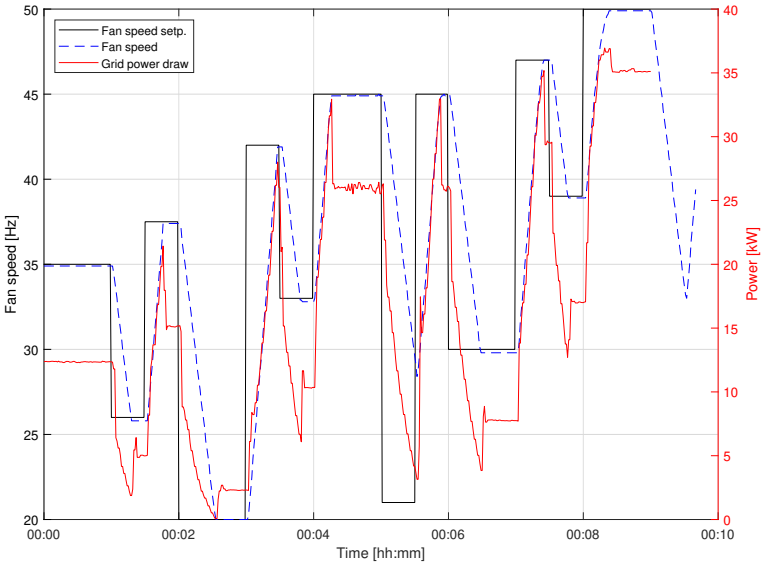

Figure 3.3 Power and speed measurements from fan test at Väla.

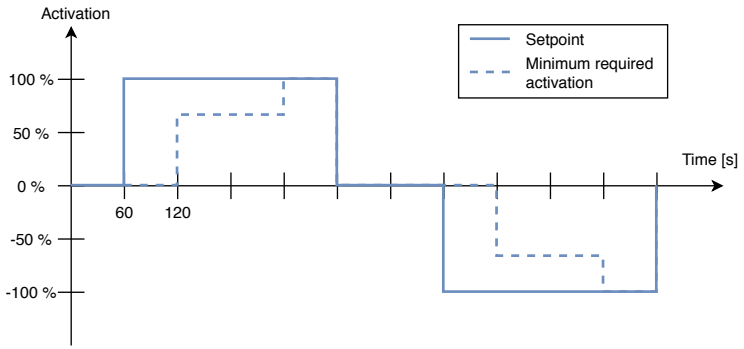

Figure 3.4 Time response requirements for FCR-N participation.

Flexibility Function, F1
Input 1: Grid frequency [Hz], Input 2: Maximum Power Flexibility [kW].
Output: Balancing Power [kW].
To simulate a grid frequency signal, we imported historical frequency data, sampled at 10 Hz, to Matlab and replayed it as time series data during simulation. We fed the grid frequency and the maximum power flexibility as inputs to F1 in order to determine the amount of power to add or subtract from the nominal power setpoint. This function is described in Section 2.1 where 100 % activation corresponds to maximum power flexibility. During simulation, we set the maximum flexibility to 4.8 kW, corresponding to 40 % of nominal fan power.

3.3 Ventilation System Model - System 1

The modelling presented in Section 3.2 is in this section extended to cover modelling of the duct system and room automation. We modelled these parts of the system to simulate a real-world system without modifications. After this section of modelling, a ventilation system model capable of flexible power consumption using standard room automation has been implemented. This model is denoted as System 1, see Figure 3.2. The purpose of this model was to serve as the base building block when developing control strategies to improve the behaviour of the ventilation system during frequency containment. We used the Simscape fluids library [MathWorks, 2020b] for modelling and simulation.

Duct System

System Operating Point, P2
Input 1: System Resistance [m^2], Input 2: Fan Speed [Hz].
Output 1: Pressure [Pa], Output 2: Flow [m^3/s].
Varying the flow area by closing or opening VAV dampers directly effects the system resistance curve. This is reflected as Input 1 and is modelled by the library using air flow channels. To model how fan speed translates to duct pressure and air flow, we used a fan block [MathWorks, 2020a] from the Simscape fluids library. Using this block required the creation of fan curves for several rotational speeds to define the behaviour of the fan. We approximated the typical look of fan curves presented in Figure 2.2 by linear functions as seen in Figure 3.5. This approximation was motivated by the fact that system operation was constrained between the minimum and maximum system resistance curves. Since a ventilation system poses constraints on the system resistance, the situation of no flow or no pressure was never reached. The system operates in a region enclosed by the intersection of fan curves and system resistance curves for minimum and maximum fan speed and system resistance respectively.

Non-linear fan curves were tested but did not alter system behaviour when compared to linear fan curves. They only made the process of tuning the model more

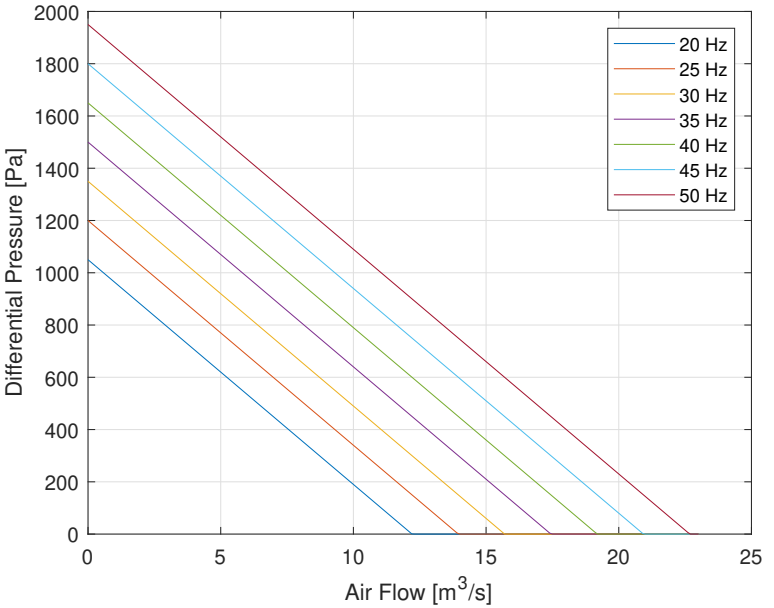

Figure 3.5 Fan curves for the fan system operating point block, P2.

time consuming. We therefore decided to use the linear approximation.

To tune the fan curves, we performed a second test at Väla. The test was performed on the system shown in Figure 2.4. During this test, we issued steps to the pressure setpoint, allowing the AHU cascade control system to operate while measuring the fan speed and the duct pressure. In simulation, we measured the duct pressure directly after P2, as seen in Figure 3.2, in contrast to the real-world system where the exact sensor location was unknown. Hence, we made an assumption to disregard the absolute values of the pressure from the real world test, and focus on replicating the dynamic behaviour. We logged the pressure range of the simulated model and scaled the real world test pressure data to match this interval. The fan curves were tuned so that the dynamic behaviour of the simulated duct pressure matched that of the measured duct pressure. The results and the comparison are shown Figure 3.6.

Duct, P3

Input 1: Pressure [Pa], Input 2: Air flow $[m^3/s]$.
Output 1: Pressure [Pa], Output 2: Flow $[m^3/s]$.
As air travels through duct work, it loses pressure due to viscous friction losses. We modelled this using pipes from the fluids library between each room. We set the pipe lengths to 27 m between the fan and the first room and 1.5 m between consecutive rooms. These values accomplished the goal of simulating pressure drops between

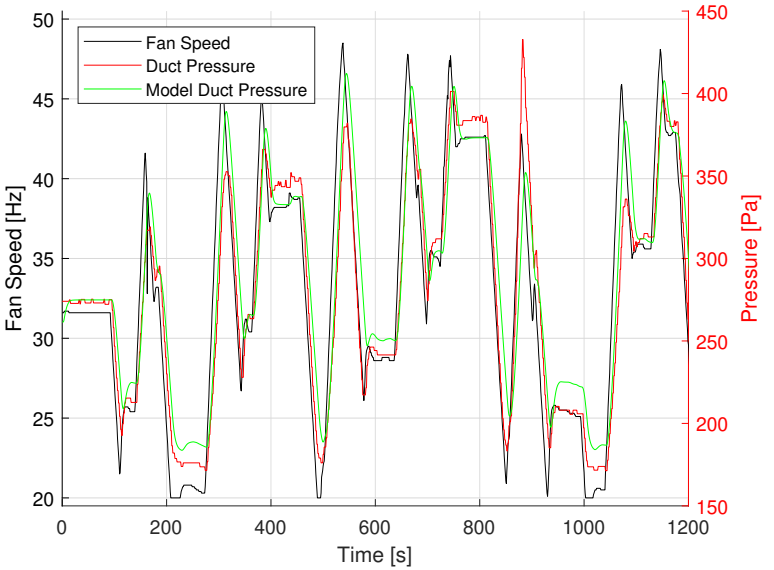

Figure 3.6 Comparison of response from fan speed (black) to duct pressure for real-world test (red) and simulated duct pressure (green).

rooms. We set the cross-sectional area of the pipes to 0.5 m^2.

Room Automation

Throughout simulation, we used a set up of three rooms connected in parallel to the duct. We chose this number in order to reveal upstream and downstream effects rooms may have on each other. This could have been accomplished using any number of rooms, larger than one. The subsystems of each room, seen in Figure 3.2, are elaborated.

Damper, P4
Input: Damper area setpoint [m^2].
Output: Damper area [m^2].
We assumed the damper to be a system with limited rate of change and having a minimum and maximum area. Furthermore, we assumed that dampers could adjust the inlet area from minimum to maximum and vice versa in 100 seconds [Swegon, 2019], deciding the slew rate. The restricted area of the dampers was set to operate within 0.4-2 m^2, simulating the full inlet of a room. We used the previously mentioned fluids library for the implementation, dividing the total area of each room inlet amongst four variable local restrictions, allowing each to control its area in the range 0.1-0.5 m^2.

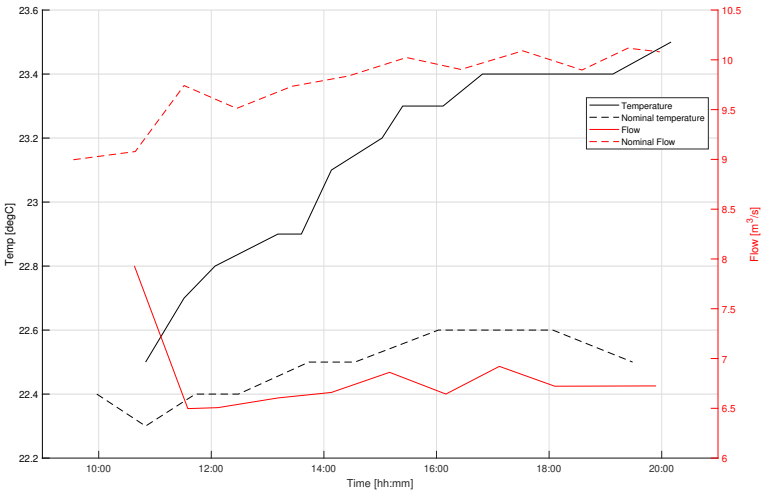

Figure 3.7 Temperature measurement from a Väla store while subject to nominal fan operation (dashed) and the fan operating at minimum speed (solid). The fan was set to minimum speed between 10:37 am and 8:00 pm. The sampling was limited by the Väla BMS and therefore varied between tests.

Flow, P5

Input 1: Pressure [Pa], Input 2: Damper area [m^2].
Output: Air flow [m^3/s].
We assumed the air flow into rooms to instantly change upon changing the inlet area or duct pressure. Hence, no dynamics were modelled for the flow specifically. We decided the nominal flow into each room by setting the fan power setpoint to 12 kW while holding the damper area locked in the middle of its operating range. The total air flow in the duct divided by the number of rooms was about 4.7 m^3/s. We chose this value as the flow reference to each room. Dimensioned room air flows at Väla ranges from 1-10 m^3/s.

Temperature, P6

Input: Air flow error [m^3/s].
Output: Temperature deviation [$^\circ C$].
To develop an understanding of the temperature dynamics, we performed a test on a section of Väla supplied by two AHUs. The test was conducted by overriding the fan speed setpoint, setting it to the minimum rotational speed, 20 Hz, during a full day while measuring the change in temperature. The nominal rotational speed of the fan was 35 Hz. We logged temperature measurements in a store with a floor area of 1250 m^2 and compared the results to a day of nominal operation, see Figure 3.7.

We modelled the dynamic behaviour of the temperature by feeding the flow error through a first order transfer function, where a decrease in flow lead to an

increase in temperature and vice versa. Supported by the result seen in Figure 3.7, we estimated the time constant and gain for the transfer function. The room in which the test was conducted was large compared to other rooms at Väla. Therefore, we assumed that the temperature increase in other rooms may be larger than shown in Figure 3.7. We then performed the minimum fan speed test in simulation by setting the fan to its lowest possible speed of 20 Hz while fixing dampers in the middle of their operating range. This resulted in a flow error of each room of approximately 1.2 m^3/s. We chose the parameters of the transfer function conservatively, so that this flow error produced a time constant of 3 hours and a temperature change of 2.5 $^\circ C$, resulting in the transfer function $\frac{2.5/1.2}{10800s+1}$.

Temperature Controller, C2 & Flow Controller, C3
C2 Input: Temperature error [$^\circ C$], C3 Input: Flow error [m^3/s].
C2 Output: Air flow setpoint [m^3/s], C3 Output: Damper setpoint [m^2].
We tuned both the temperature controller C2 and the flow controller C3 without reference test data. We based the tuning on a response to a 1 $^\circ C$ temperature step disturbance added to the temperature measurement signal of the first room. We assumed that such a step disturbance has a settling time of roughly 90 minutes. The controllers were tuned to match this assumption.

3.4 System Evaluation

Until this point we have modified the base system presented in Figure 2.4 as little as possible to allow for frequency containment, resulting in System 1 shown in Figure 3.2. In this section, tests are presented that will allow for evaluation of system performance. We used these tests to identify potential problems with performing frequency containment on System 1, as well as to evaluate performance for System 2 and 3 developed in Sections 3.5 and 3.6.

Tests

We assumed room temperature deviation to be a limiting factor when performing frequency containment. These tests would show system behaviour as well as room temperatures when subject to real frequency data, as well as step responses and disturbance tests.

Test 1 - Frequency Containment
During Test 1 we used real frequency data, sampled at 10 Hz, as the input to the model for ten hours. The purpose of this test was to give an idea of how room temperature and reference signal tracking behaved when subject to real frequency data. Hence, power setpoint, power consumption and room temperatures were logged. We performed this test using historical frequency data from 2018-12-28, the distribution of which is shown in Figure 4.2.

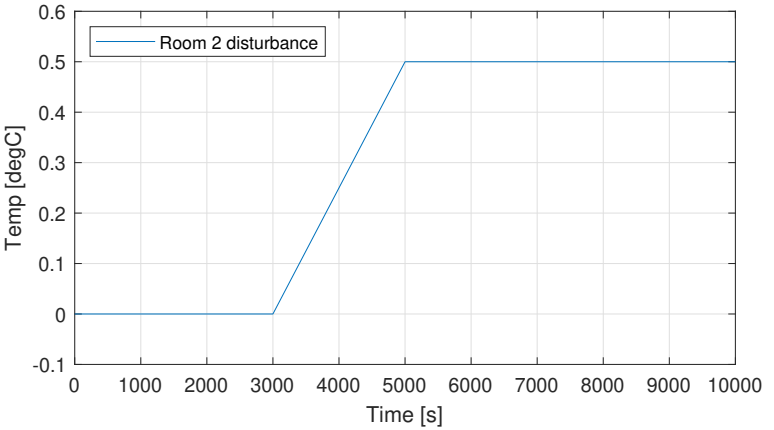

Figure 3.8 Ramp temperature disturbance for test 3.

Test 2 - Frequency step response
The purpose of Test 2 was to investigate how duct pressure and room temperatures were affected during periods of very high or low frequency. In this test we changed the frequency signal in steps. First, we set the frequency to 50.1 Hz for 5 hours, then to 50 Hz to let the system reset, then to 49.9 for 5 hours. We logged duct pressure, room temperatures and VAV areas.

Test 3 - Temperature Disturbance
The purpose of Test 3 was to evaluate the system performance with regards to a disturbance. We set the fan to operate at nominal power and issued a disturbance which was chosen to be a temperature ramp, see Figure 3.8. We added it to the temperature error of the second room whilst logging room temperatures and VAV damper areas.

3.5 Room Automation Control Strategy - System 2

After performing tests 1, 2 and 3 on System 1, we noticed that the room automation behaved in an undesirable manner. This behaviour manifested itself in high duct pressure levels due to VAV dampers closing at high power consumption. Also, at low power consumption, the room farthest downstream was starved of air flow, resulting in a temperature increase. We aimed further development at improving the behaviour of the system, reducing these problems. System 2 featured a simple control structure in which dampers were locked during frequency containment. Figure 3.9 shows a block diagram of the suggested control strategy. The modifications compared to System 1 are further elaborated.

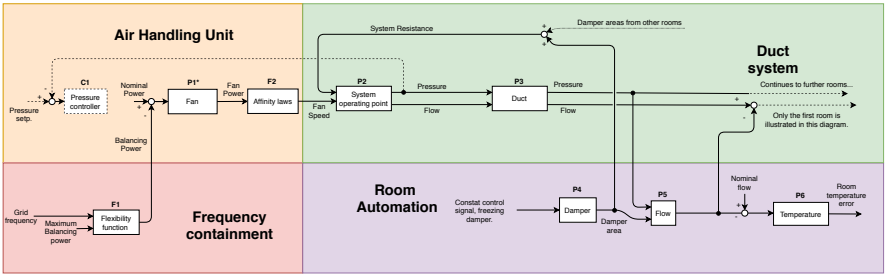

Figure 3.9 Block diagram illustrating the strategy of System 2. VAV dampers were frozen to reduce duct pressure peaks and air flow imbalances between rooms.

Room Automation

Damper, P5

The dampers were held at a constant area while frequency containment was active. We did this to decrease the system resistance compared to a system where dampers closed as a response to high air flow. We thought that this would reduce air flow imbalances between rooms and, in extension, the temperature difference.

Requirements

For this strategy to be applied in reality, it is required that room automation and fan control signals are mutable. Also, as for all frequency containment applications, the grid frequency must be measured.

3.6 Room Automation Control Strategy - System 3

Locking dampers, as in System 2, had a few drawbacks. It was a static solution, completely eliminating the purpose of VAV dampers since air flow was no longer controlled actively. Also, there was no ability to suppress disturbances. The strategy presented in System 3 aimed to preserve dynamic behaviour whilst alleviating the problems with System 1. The resulting strategy is shown in Figure 3.10 and the changes compared to System 1 are further elaborated.

Duct System

P-controller, C4

Input: Positive duct pressure error [Pa].
Output: Air flow feed forward $[m^3/s]$.
When changing the fan control loop from pressure controlled to power controlled, duct pressure control authority was greatly reduced. However, it was still possible to reduce pressure by altering the system resistance. Hence, as a safety precaution

for high duct pressures we added an extra control loop, C4. This controller is active only if the duct pressure rises above a predetermined duct pressure threshold. During simulation, we set this threshold to 300 Pa as this was slightly lower than the maximum duct pressure. 300 Pa is most likely not enough to cause any significant damage in a real system, but it was chosen to illustrate the working principle of the added controller. Real systems at Väla reached upwards of 1 kPa without danger. The controller added a term to the air flow setpoint of each room, as in Figure 3.10, opening the dampers to reduce duct pressure. We implemented the controller with a gain of 0.3.

Room Automation

To balance the air flow and temperature between rooms, we developed a system for load distribution as follows: When a situation of low air flow occured in a room, the room communicated positive air flow and temperature errors upstream to the next room in the chain of rooms. Example: If a flow error was present in room 2, this error was subtracted from the setpoint in room 1, resulting in room 1 demanding less flow, see Figure 3.10. This propagates upstream from the end of the ventilation system until all rooms share the load. When a situation of high air flow occurs, an inverted version of the strategy was applied. Negative air flow and temperature errors were communicated downstream instead of upstream. This is excluded from Figure 3.10 for clarity but was implemented during simulation. Furthermore, we theorized that this strategy did not have to be applied to an entire ventilation system but could be used to alleviate the load in certain rooms more exposed to starvation or excessive air flow. Also, it allows for disturbance rejection since normal VAV operation is preserved.

Requirements

System knowledge or testing is required to identify rooms prone to starvation. Also, in a real system, all rooms do not have the same nominal air flow. Hence, tuning may be required in order to feedback a reasonable proportion of the air flow and temperature errors.

3.7 System Models Summary

This chapter covered the process of system modelling. First, we created System 1 by applying flexible power consumption to the fan of a VAV system. No changes were made to the room automation. System 1 had problems with high maximum duct pressure levels and starvation of air flow in to rooms.

We proceeded to develop System 2 as a simple solution to these problems. The modification compared to System 1 was to lock dampers in place during flexible power consumption. This lowered the maximum duct pressure levels and created

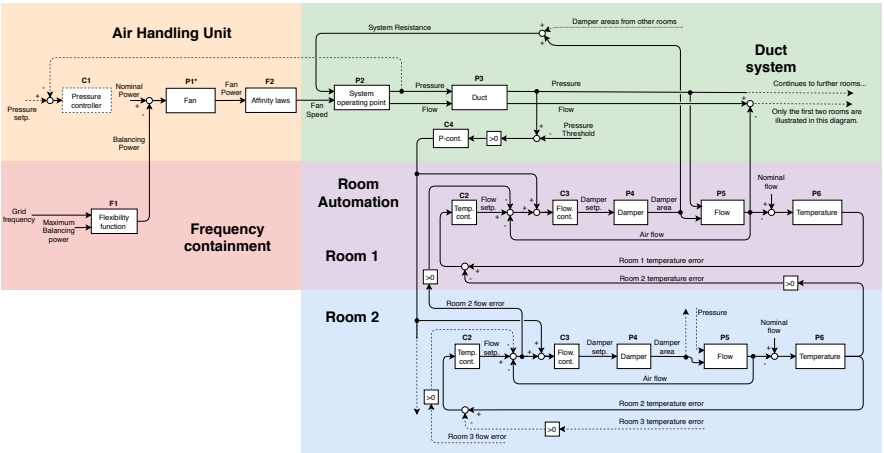

Figure 3.10 Block diagram illustrating the control structure of System 3. Load distribution and duct pressure control was implemented.

more balance in the air flow between rooms. However, by locking dampers we eliminated VAV functionality. Also, the maximum duct pressure level was not controlled to a specified level even though it was reduced.

Due to the flaws of System 2, we developed System 3 with some key goals in mind: retaining VAV functionality, actively controlling pressure and reducing the air flow imbalance between rooms. Maximum pressure levels were controlled by adding a P-controller to open VAV dampers if a pressure threshold was exceeded. Air flow was balanced between rooms by communicating flow and temperature errors upstream or downstream depending on the sign of the error.

4

Result

4.1 Data Analysis

Frequency Data Analysis

What follows are the results from the frequency data analysis. To get an overview of the general behaviour of the grid, the grid frequency distribution of 2019 is shown in Figure 4.1. The grid frequency mostly reside inside the FCR-N area, 49.9-50.1 Hz. It is also clear that there is no apparent weight towards higher or lower frequencies. The frequency is, on a yearly scale, normally distributed around 50 Hz. When analysing frequency distribution of shorter time periods, such as single days, the distribution can vary greatly. Figure 4.2 shows the distribution of the two days with the highest and lowest average frequency during Välas opening hours, 10 am-8 pm. These distributions are scenarios that DRRs are expected to comply with.

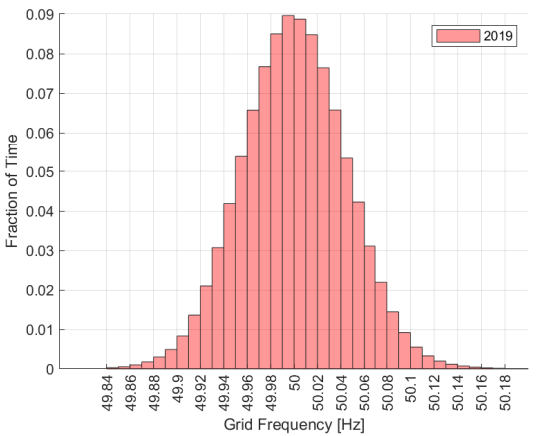

Figure 4.1 Grid frequency distribution during 2019.

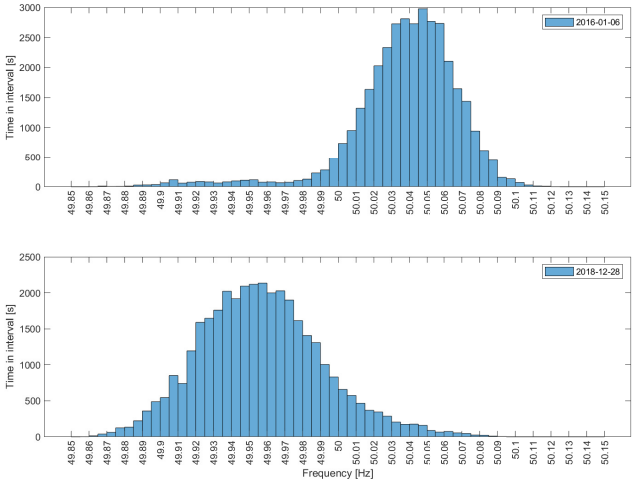

Figure 4.2 Distributions from the two extreme cases of average frequency during daytime between 10am-8pm.

Economical Analysis

The results from the economical analysis are shown in Figure 4.3. We showed that is was more beneficial to participate on FCR-N during nighttime when day and night time were defined as in the figure. This was due to the FCR-N price typically being higher during night time for the years in question. Also, besides the revenue gained from FCR-N, the electricity bill changed when DRR was provided. This change in cost was a few percent of the revenue earned as shown in the figure and did, on a yearly average, result in savings during nighttime and an increase in cost during daytime. This was due to the frequency being, on average, higher during daytime and lower during nighttime.

As an example, Väla was assumed to have a capacity of 0.2 MW of balancing power from ventilation fans. This would have yielded a revenue of about 17 000 EUR during 2019, judging from the result in Figure 4.3 and assuming participation on FCR-N during open hours 10 am-8 pm.

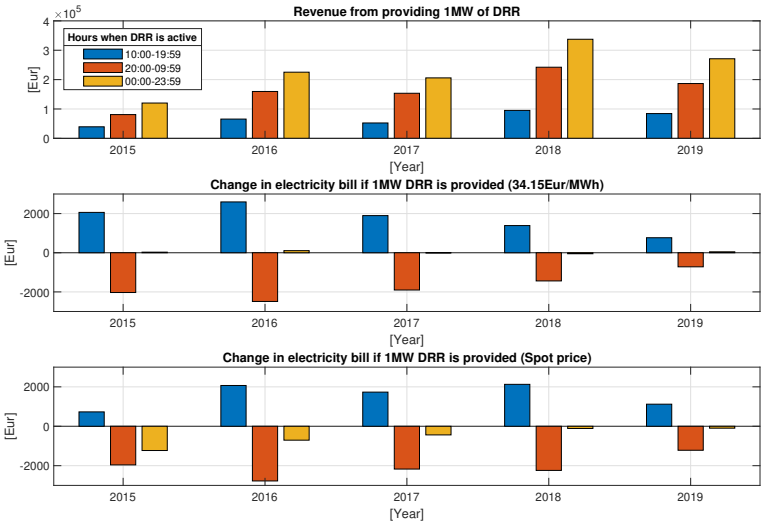

Figure 4.3 Revenue and change in electricity bill if DRR is provided. The constant MWh price is based on the average spot price during the period 2015-2019.

4.2 System Evaluation

This section presents the evaluation of the simulated systems by presenting results from the tests described in Section 3.4.

System 1

Test 1 - Frequency Containment

The results from Test 1 are shown in Figures 4.4 and 4.5. Figure 4.4 shows that the power consumption tracks its reference value well. Figure 4.5 shows the room temperature response to a full day of frequency containment. From these results, it is clear that room 3 was exposed, being starved of air flow.

Test 2 - Frequency step response

The results from Test 2 are shown in Figure 4.6. These results were used to identify the problems that arise when flexible power consumption was added to a ventilation system. As grid frequency increased, duct pressure rose due to the increase in power consumption. Also, due to the excessive air flow, VAV dampers closed which further increased duct pressure. The first room suffered a decrease in temperature due to its position along the duct. As grid frequency decreased, the last room suffered an increase in temperature due to the rooms upstream claiming more of the total flow. This is similar to the behaviour shown in Figure 4.5.

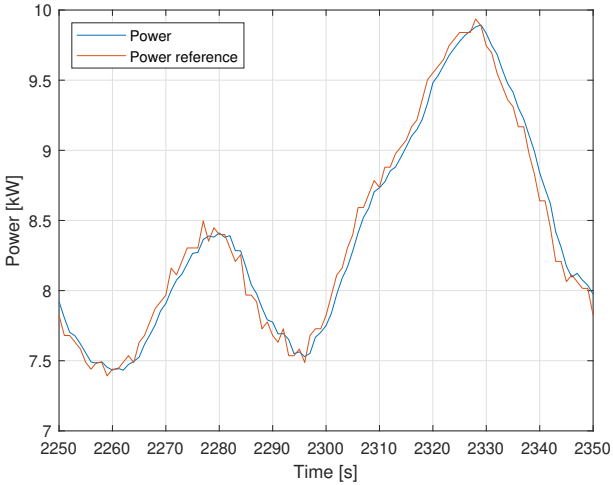

Figure 4.4 Snapshot of the simulated power reference tracking from Test 1.

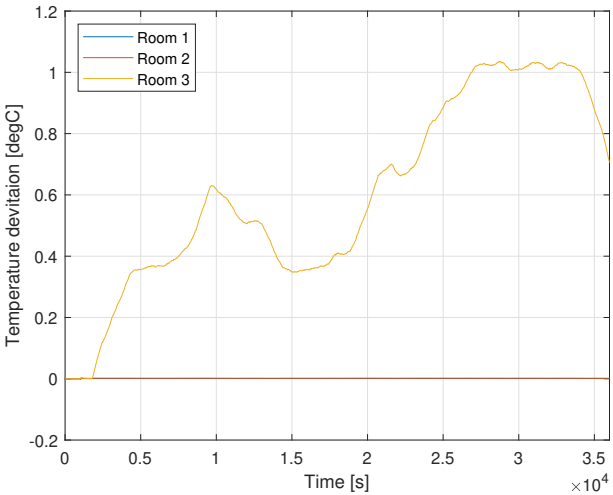

Figure 4.5 Room temperature deviation of System 1 while subject to Test 1. Room 1 and 2 kept their desired temperatures while room 3 could not maintain sufficient flow and therefore suffered an increase in temperature.

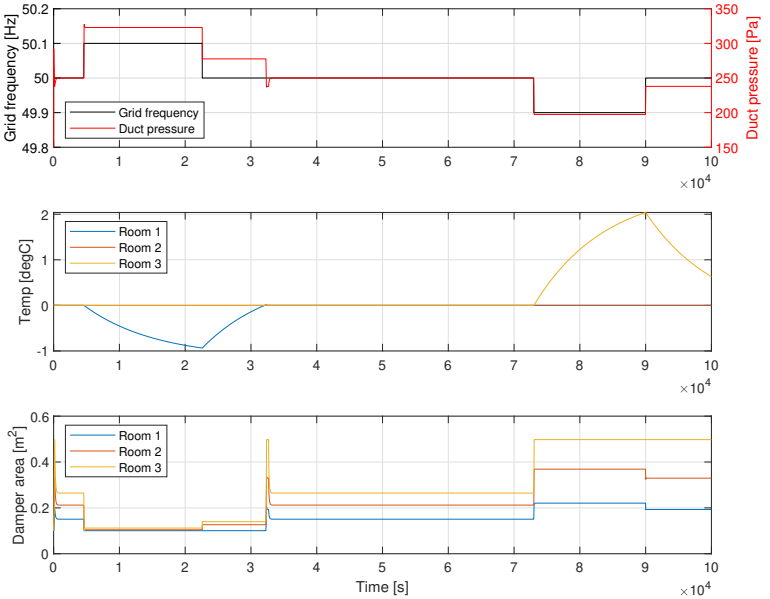

Figure 4.6 Results from Test 2 on System 1. As grid frequency increased, duct pressure rose due to the increase in power consumption (upper plot). The damper area responded (lower plot) to maintain desired air flow. When grid frequency increased, only the first room deviated from its desired room temperature and when grid frequency decreased, only the third room deviated from its desired room temperature (middle plot).

Test 3 - Temperate Disturbance

The results from Test 3 are shown in Figure 4.7. As the system was no longer controlled with the priority of supplying air to rooms, but to provide flexible power consumption, there was no authority to increase the flow to fully suppress the disturbance. The damper of room 2, in which the disturbance was present, opened in order to cool the room down. This resulted in room 2 claiming more of the total flow, starving room 3, the damper of which opened fully.

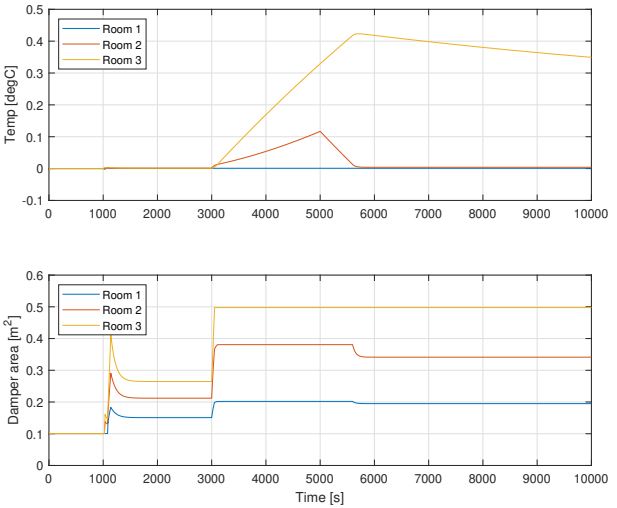

Figure 4.7 Results from Test 3 on System 1. As the temperature disturbance was introduced, the damper areas increased to increase flow and to lower temperature. This caused starvation of room 3 resulting in the temperature deviation being shifted from room 2 to room 3.

System 2

Test 1 - Frequency Containment

System 2 featured a strategy to reduce the problems of System 1. The power reference tracking results are the same as for System 1, see Figure 4.4. The room temperature results are shown in Figure 4.8. These results show that the temperature deviation is distributed more evenly amongst the rooms, however not completely balanced.

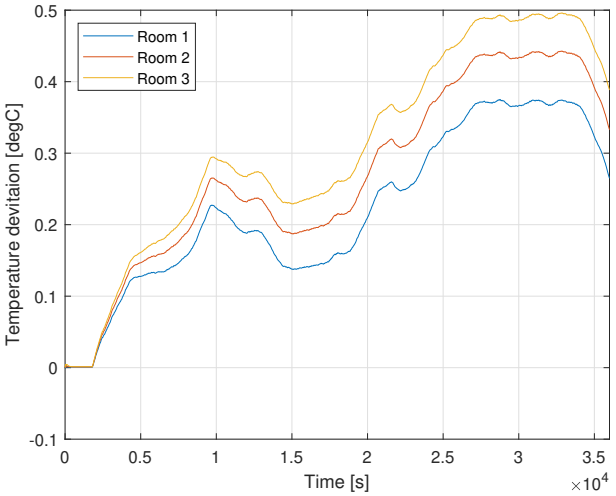

Figure 4.8 Results from Test 1 on System 2. As dampers were locked, the rooms suffered similar temperature deviations.

Test 2 - Frequency step response

The results from Test 2 are shown in Figure 4.9. Comparing these results to the corresponding tests on System 1, in Figure 4.6, duct pressure peaks are lower and room temperatures are more balanced.

Test 3 - Temperate Disturbance

The results from Test 3 are shown in Figure 4.10. System 2 had no ability to suppress disturbances due to its static nature.

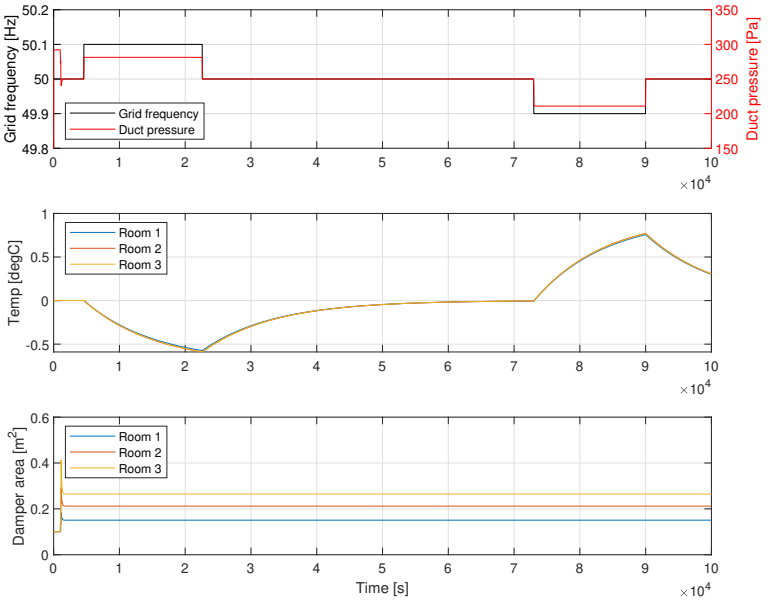

Figure 4.9 Results from Test 2 on System 2. As grid frequency increased, duct pressure rose due to the increase in power consumption (upper plot). The pressure increase was smaller when compared to System 1 since the dampers did not close (lower plot). The temperature deviation was almost identical in all the rooms (middle plot). The damper behaviour at the start of the test was a result of allowing the system to reach steady state before freezing the dampers.

System 3

Test 1 - Frequency Containment

The power reference tracking results are the same as for System 1 and 2, see Figure 4.4. The room temperature results from Test 1 are shown in Figure 4.11. The temperature deviation was in this case more balanced, evenly distributed amongst rooms.

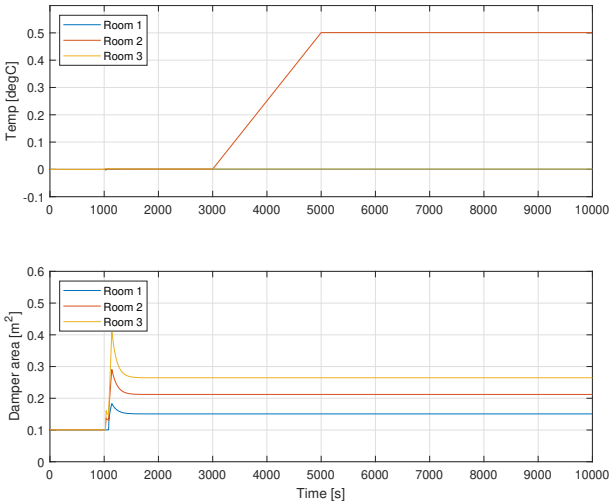

Figure 4.10 Results from Test 3 on System 2. Since the dampers were locked in position, the system had no way of suppressing the disturbance (upper plot). Room 1 and 3 were unaffected by the disturbance. The damper behaviour at the start of the test was a result of allowing the system to reach steady state before freezing the dampers.

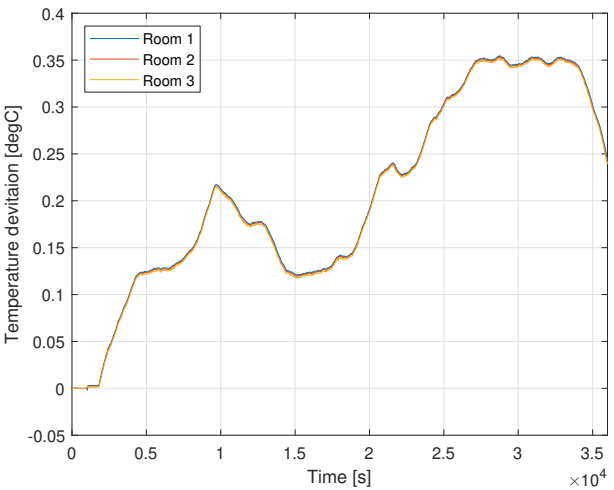

Figure 4.11 Results from Test 1 on System 3. The temperature deviation was evenly distributed amongst the rooms.

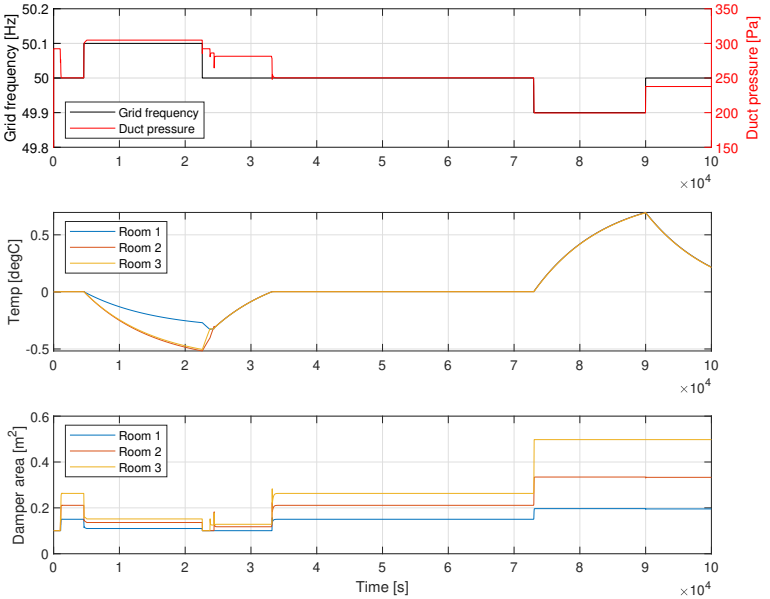

Figure 4.12 Results from Test 2 on System 3. As grid frequency increased, duct pressure rose due to the increase in power consumption (upper plot). The pressure only marginally increased over the 300 Pa threshold. The temperature deviation was almost identical in all the rooms (middle plot), except for the time period when the pressure was above the threshold. VAV dampers actively contributed (lower plot) to distribute the load across all rooms.

Test 2 - Frequency step response

The results from Test 2 are shown in Figure 4.12. The system was actively operating to balance the air flow and temperature deviation in the rooms which can be seen in the damper area plot. This showed that dynamic behaviour was preserved when this strategy was applied.

Test 3 - Temperate Disturbance

The results from Test 3 are shown in Figure 4.13. This figure shows one clear benefit to this strategy: The disturbance was suppressed by the system and the temperature load was distributed amongst the rooms.

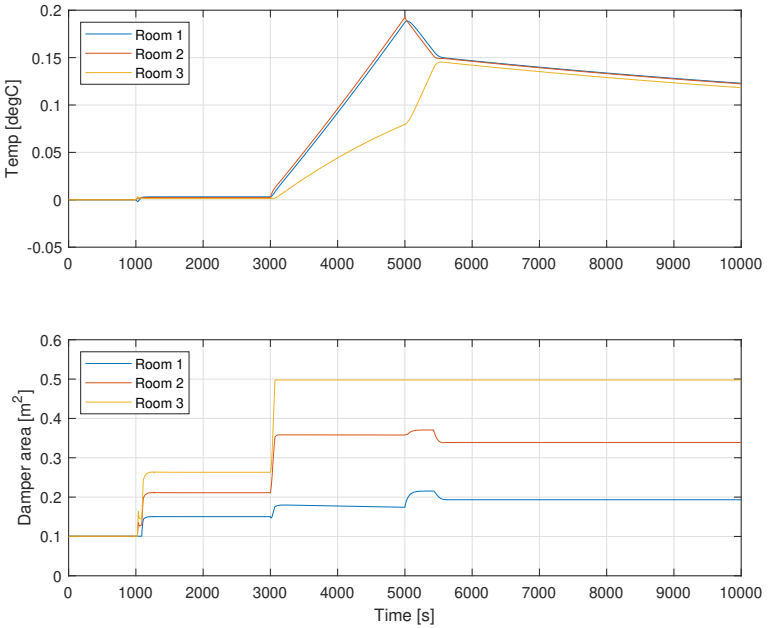

Figure 4.13 Results from Test 3 on System 3. The temperature disturbance was evenly distributed between the room that was subject to the disturbance and its upstream neighbour.

5

Discussion

5.1 Key Findings

We have shown that ventilation fans meet the requirements to participate on FCR-N. We developed a generic VAV ventilation system model for simulating system behaviour. When applying flexible power consumption and frequency containment to a VAV ventilation system, undesirable behaviour regarding the room automation was found. We identified and visualised problems related to duct pressure levels and room air flow imbalances. Room automation control strategies were developed in order to reduce these problems. We showed that simple control strategies (System 2) can reduce problems significantly and that further developed strategies (System 3) can be used to better control duct pressure and minimize temperature deviation whilst performing frequency containment. Improved room automation performance allows for larger power flexibility for ventilation fans assuming that indoor climate metrics and duct pressure are the limiting factors.

5.2 Project Delimiters

We focused on VAV systems since they are relatively complex when compared to other ventilation systems. As VAV systems reside in various configurations, we disregarded detailed system implementations and complex modelling techniques in favour of analysing VAV systems in a generic manner. This was important for the thesis results to be applicable to a wider range of VAV systems. Due to this approach, the results from this thesis would need adjustments and testing before being applied to a real world system.

5.3 Assumptions & Simplifications

Power Measurement

To control power consumption for setpoint tracking in real time, we assumed power consumption of the fan to be measurable. The power consumption of a real world

ventilation fan depends on many parameters such as the operating point of the fan, filters, efficiency of the motor and degradation of parts. We deemed this as a subtopic of too large magnitude for the thesis. Also, it was very likely that power estimation, in the Väla project, would be done by explicitly measuring the power consumption, motivating the assumption further.

Simulated Power Consumption

We modelled the simulated power consumption dynamics as P1*. As the system operating point, P2, required a fan speed as an input, the fan power consumption was converted to a speed using affinity laws. In reality, power consumption is also affected by VAV dampers: As they move they alter the operating point of the fan leading to a change in power. As fan power consumption varied greatly whilst performing frequency containment, the slight impact from VAV dampers was neglected.

Indoor Climate

Temperature and CO_2 levels are the two primary metrics for evaluating indoor air climate. As ventilation systems are primarily used for cooling purposes, we used indoor temperature as a metric to evaluate effects on indoor climate. From internal sources at Siemens, experience stated that temperature was a good indoor climate metric as it typically deviates prior to CO_2 levels.

Simulated System Structure

In simulation, we used a simplified ventilation system, only containing three rooms. This number was deemed to be small enough to be feasible for simulations, whilst giving enough insight into the down and upstream effects between rooms. Also, a more complex system with branching duct works and many VAV controlled rooms could, in theory, be simplified to a less complex, equivalent system, motivating the validity of the model.

5.4 Control Strategy Evaluation

System 1

System 1, where flexible power consumption was implemented without considering room automation, showed problems with duct pressure peaks and imbalances between rooms. In a real world system, duct pressure peaks may reach magnitudes harmful to the system. Also, starving rooms of fresh air for prolonged periods of time gave rise to temperature increases in exposed rooms. These results were a consequence of the VAV room automation control structure. Specifically, the closed control loop of the air flow was fast and reacted quickly to changes in fan power, inherent to VAV systems. The possible benefit of this system was that no modifications needed to be made to the room automation.

System 2

We developed the control strategy in System 2 to reduce the problems found in System 1. This solution has the potential to require little effort and economical investment during implementation in a real world system since it revolves around locking dampers in place. Also, since the system resistance was held constant, it could be possible to get an estimate of the power consumption, without explicitly measuring it, using affinity laws. However, the implementation of System 2 was static, locking damper areas, which made it prone to disturbances and varying temperature loads. It eliminated the entire purpose of VAV control, since air flow was no longer actively controlled.

Another option, besides fully locking dampers, could have been to only control the damper with regards to room temperature, removing the inner air flow control loop from the room automation in Figure 3.2. This would make the control loop much slower, making it more resilient towards fast changes in grid frequency. The drawback would be that accurate control of air flow would be lost. We did not implement this.

System 3

The main purpose of VAV systems is to dynamically control air flow. System 3 was implemented to balance air flow between rooms and to control the duct pressure whilst retaining VAV functionality. It also responded dynamically to disturbances. We theorized that the strategy was generic and applicable to VAV systems independent of the specific system layout. It used a low amount of signals and simple arithmetic operations in its implementation. Drawbacks of the system could be that it is not always clear what rooms are most exposed to starvation or excessive air flow. For this reason this strategy is slightly more complicated than System 2. However, in a real world scenario, it may not be necessary to implement this strategy across an entire system. The strategy can be limited to exposed rooms or areas by distributing their load amongst other rooms with a larger tolerance or a larger nominal air flow, reducing the implementation complexity and cost.

6

Conclusion

The goal of this thesis was to investigate the implications of flexible power consumption for ventilation fans in variable air volume (VAV) systems. The purpose was for the fan to act as a balancing resource for the grid. We built ventilation system models in Simulink to identify potential problems as well as to further develop the control strategies for the system. We showed that implementing flexible power consumption without considering room automation effects had many flaws such as high duct pressure levels and imbalances in air flow to rooms, starving or producing excessive air flow in to exposed rooms. We developed two room automation control strategies of varying complexity to facilitate flexible power consumption and to reduce the aforementioned problems. The first strategy presented (System 2) revolved around locking VAV dampers. This greatly reduced the previously mentioned problems and may, in some cases, be enough of a solution. The final, and recommended, solution featured load distribution as well as a control loop to handle duct pressure levels (System 3). The purpose of the load distribution was to evenly distribute the flow and temperature errors amongst the affected rooms. This strategy allowed for normal VAV operation and flexible power consumption whilst greatly reducing the temperature deviations and controlling duct pressure.

When implementing these strategies in real world systems, there needs to be preparatory work to identify limitations with regards to duct pressure, exposed rooms and power flexibility. As shown in the results, the economical potential is limited, requiring the investment cost to be kept as low as possible to ensure economical feasibility. System 3 is only marginally more complex than System 2 while retaining VAV functionality. It is therefore the recommended solution. However, should the system be able to operate without VAV functionality, System 2 can be used during hours of flexible power consumption allowing for a simpler, more cost effective implementation.

7

Future Work

Power Flexiblity and Bidding Strategy

Resources acting as DRRs need to contribute with a specific amount of power flexibility. Deciding this amount is not a trivial task. Besides the maximum and minimum power consumption values, there are multiple parameters that can be chosen as limiting factors to the flexibility such as indoor climate, sound levels and pressure levels. Also, one ventilation fan is not enough to meet the volume requirements for participation on FCR-N. Hence, a participating resource is usually an aggregation of smaller units, complicating matters further as there is a need to control multiple units in unison.

Estimating Power Consumption

During this thesis, we deemed power measurement necessary in order to reliably track a power reference. When systems using power measurement are operational, the potential exists to store sensor data using BMS systems. Data driven methods can then be used to estimate power consumption without explicit measurement. We based this suggestion on the fact that Väla features a lot of sensor measurements but has no measurement of power.

Other DRRs

Besides ventilation fans, other systems have the potential to act as DRRs. Batteries, solar panels, heat pumps and chillers are some potential candidates for flexible power consumption and generation.

Bibliography

Energimyndigheten (2019). *Energiläget 2019*. https://energimyndigheten.a-w2m.se/Home.mvc?resourceId=145396. [Online; accessed 18-February-2020].

Fingrid (2020). *Frequency - historical data*. https://data.fingrid.fi/en/dataset/frequency-historical-data. [Online; accessed 20-February-2020].

Iggström, D. and P. Svensson (2019). *Demand-side flexibility in shopping centres - A case study on Väla shopping centre*. MA thesis. Lund University, Sweden.

MathWorks (2020a). *Fan (g)*. URL: https://se.mathworks.com/help/physmod/hydro/ref/fang.html?s_tid=srchtitle (visited on 2020).

MathWorks (2020b). *Simscape fluids*. URL: https://se.mathworks.com/products/simscape-fluids.html#fluid-power (visited on 2020).

McLoone, J. (2019). *Fan performance and fan laws*. https://fluidflowinfo.com/fan-performance-and-fan-laws/.

NEPP (2016). *Reglering av kraftsystemet med ett stort inslag av variabel produktion*. http://www.nepp.se/etapp1/pdf/reglering.pdf. [Online; accessed 18-February-2020].

Nordpool (2020). *Historical market data*. https://www.nordpoolgroup.com/historical-market-data/. [Online; accessed 25-February-2020].

Persson, V. (2019). *Virtual power plant contributing to primary frequency containment using demand response*. MA thesis. Lund University, Sweden.

Siemens and Väla (2020). *Väla bygger sveriges första virtuella kraftverk i samarbete med siemens*. http://www.mynewsdesk.com/se/vala/pressreleases/vaela-bygger-sveriges-foersta-virtuella-kraftverk-i-samarbete-med-siemens-2977902. [Online; accessed 20-April-2020].

SvK (2018). *Overview of the requirements on reserves*. https://www.svk.se/siteassets/aktorsportalen/elmarknad/information-om-reserver/reserve-markets.pdf. [Online; accessed 17-February-2020].

SvK (2019). *Upphandling av frequency containment reserve (fcr) januari – december 2020*. https://www.svk.se/press-och-nyheter/nyheter/elmarknad-allmant/2019/upphandling-av-frequency-containment-reserve-fcr-januari--december-2020/. [Online; accessed 18-February-2020].

SvK (2020a). *Organization*. https://www.svk.se/en/about-us/organization/. [Online; accessed 20-March-2020].

SvK (2020b). *Primärreglering*. https://mimer.svk.se/PrimaryRegulation/PrimaryRegulationIndex. [Online; accessed 25-February-2020].

SvK (2020c). *Villkor för fcr*. https://www.svk.se/siteassets/aktorsportalen/elmarknad/balansansvar/dokument/avslutad-remiss-4620/5-bilaga-3-fcr.pdf. [Online; accessed 20-March-2020].

Swegon (2019). *React*. URL: https://www.swegon.com/globalassets/_product-documents/flow-control/demand-controlled-ventilation/_en/reacta.pdf (visited on 2019).

Toolbox, E. (2003). *Fan affinity laws*. https://www.engineeringtoolbox.com/fan-affinity-laws-d_196.html. [Online; accessed 20-April-2020].

Vattenfall (2019). *Tjäna pengar på din flexibla elförbrukning*. https://energyplaza.vattenfall.se/blogg/var-bland-de-forsta-i-sverige-att-tjana-pengar-pa-din-flexibla-elforbrukning. [Online; accessed 25-February-2020].

Lund University
Department of Automatic Control
Box 118
SE-221 00 Lund Sweden

Document name
MASTER'S THESIS

Date of issue
June 2020

Document Number
TFRT-6108

Author(s)
Ricky Klasson
Johan Frykebrant

Supervisor
Kristian Soltesz, Dept. of Automatic Control, Lund University, Sweden
Bo Bernhardsson, Dept. of Automatic Control, Lund University, Sweden (examiner)

Title and subtitle

Control Strategies for Variable Air Volume Ventilation used as a Demand Response Resource

Abstract

The Swedish power grid is actively balanced in order to maintain the nominal frequency of 50 Hz. Today, this is mostly done through flexible power generation. Emerging markets, allowing consuming resources to participate in balancing the grid, have the potential to increase the stability of the grid. This master thesis aimed to investigate the consequences and possibilities of using variable air volume (VAV) ventilation systems as a balancing resource for the grid. Through modelling and simulation of these systems, conclusions were drawn regarding the balancing potential. As a consequence of flexible power consumption, VAV room automation was negatively effected. The thesis emphasized development of generic room automation control strategies, reducing negative effects. The main outcome of this thesis was a control strategy which was able to facilitate flexible power consumption whilst retaining close to normal VAV operation. Also, a small economical analysis was performed to give an overview of the potential earnings for balancing resources.

Keywords

Classification system and/or index terms (if any)

Supplementary bibliographical information

ISSN and key title
0280-5316

ISBN

Language
English

Number of pages
1-51

Recipient's notes

Security classification

http://www.control.lth.se/publications/